Bayesian Neural Networks for Structural Damage Identification Using Time-Domain Wave Propagation Data

Bernardo Feijó Junqueira[1][0000−0002−4692−9005], Daniel Alves Castello[2][0000−0002−3010−7541], Gabriel L.S Silva[2][0009−0002−1725−9265], Rafael de O. Teloli[3][0000−0002−7658−5514], and Ricardo Leiderman[4][0000−0002−0443−9294]

[1] Rio de Janeiro State University (UERJ), Department of Mechanical Engineering, 524 São Francisco Xavier Street, Rio de Janeiro, RJ 20550-900, Brazil
bernardo.junqueira@eng.uerj.br
http://www.mecanica.uerj.br/

[2] Federal University of Rio de Janeiro (UFRJ), Department of Mechanical Engineering, Rio de Janeiro, RJ, Brazil
castello@mecanica.coppe.ufrj.br

[3] SUPMICROTECH, CNRS, FEMTO-ST, Applied Mechanics Department, 26 Rue de l'Épitaphe, Besançon, 25000, France
rafael.teloli@femto-st.fr

[4] Fluminense Federal University (UFF), Computer Science Department, Rua Passo da Pátria 156, São Domingos, Niterói, RJ 24210-240, Brazil
leider@ic.uff.br

Abstract. This study investigates the application of Bayesian neural networks for regression tasks aimed at recovering structural damage parameters from time-domain wave propagation data. The raw wave propagation data are simulated in a one-dimensional elastic bar using the Spectral Finite Element Method, considering data collection from a limited number of sensors. The damage fields are modeled as rectangular profiles, described as three parameters: position, size (or width), and magnitude. The inverse problem of damage recovery is formulated within a Bayesian framework, where the wave field data collected by the sensors serve as inputs and the output consists of probabilistic distributions of the damage parameters, allowing for quantifying uncertainty in the damage parameters, providing a stochastic characterization of the damage state. The training data includes deterministic values for system properties, while the validation and test datasets incorporate uncertainties in the elastic bar's properties, simulating modeling error for the inference stage of the inverse model. The findings of applying this approach in a structural health monitoring context are discussed, highlighting its potential in assessing structural integrity.

Keywords: Structural Health Monitoring · Deep Learning · Bayesian Neural Network · 1D Wave Propagation · Inverse Problem · Surrogate Model.

1 Introduction

Structural Health Monitoring (SHM) is an essential process for maintenance, anomaly detection, and improving the serviceability of structures through the management and repair of damage, which is often manifested by changes in mechanical properties, such as stiffness. Recently, with the fast advances of Artificial Intelligence (AI), and more specifically Machine Learning (ML) techniques, along with the adoption of Deep Learning (DL), has profoundly influenced the automation of SHM. Neural Network (NN) models have unlocked the potential for analyzing extensive datasets and intricate system behaviors through automated feature extraction. However, there are still ongoing challenges, such as the lack of interpretability regarding uncertainties in the network's output and robustness to structural changes [2], both of which are crucial for the decision-making process in an effective SHM system.

Bayesian modeling is a powerful tool for investigating uncertainty in DL models. In this context, a Bayesian Neural Network (BNN) is a NN that models uncertainties in one or more of its weights by treating them as random variables rather than deterministic entities. Therefore, a BNN provides uncertainty estimates for the network's outputs, enhancing the interpretability of the surrogate model's response [8, 4, 20]. Furthermore, BNNs can learn effectively from small and noisy datasets and are more robust to overfitting than traditional NNs. This makes them particularly suitable for applications such as SHM, where uncertainty estimates can build a cost-inform decision-making process [21]. In this regard, several studies in the literature have explored using BNNs to support SHM procedures [20, 21, 1, 24, 6, 13], with most of them focusing on damage detection, condition classification or damage evolution (severity). The exception is the work by Luo *et al.* [13], which not only detects damage but also locates it in Carbon Fiber Reinforced Polymer (CFRP) composites using ultrasonic Lamb waves, although not fully characterizing the damage profile.

The main objective of the present work is to explore the use of BNNs as a surrogate inverse model to fully characterize damage profiles using measured wave propagation data. Additionally, this study aims to address the issues and challenges associated with the proposed approach. The measured data was synthetically generated using Spectral Finite Element modeling of one-dimensional wave propagation in an elastic bar, with data collected from a limited number of sensors distributed along the bar's length. The damage profiles are modeled as rectangular shapes, fully characterized by their center position, size (or width), and magnitude. To assess the robustness of the proposed approach, the surrogate inverse model was also tested with profiles generated from a model that includes property uncertainties.

2 Mathematical Modeling

This section presents the proposed mathematical models for the forward and inverse problems, which are designed in conjunction to recover damage profiles

from time-domain wave propagation data collected in a one-dimensional elastic medium.

2.1 Forward Model - 1D Wave Propagation in an Elastic Bar

Linear elastodynamics in a one-dimensional setting (a bar) in the context of small deformations can be described by eq. (1), subjected to the appropriate boundary conditions. In this formulation, $u(x,t)$ denotes the displacement field, $E(x)$ and ρ represent the Young modulus (local) of the material and the mass density, respectively, and A is the cross-sectional area of the bar. The wave propagation phenomena can be described by eq. (1) and are nondispersive, which can be applied to bars made from linear elastic isotropic materials when lateral inertia effects are negligible [5].

$$\frac{\partial}{\partial x}\left(E(x)A\frac{\partial u}{\partial x}\right) = \rho A\frac{\partial^2 u}{\partial t^2}. \tag{1}$$

The space-discretized equations of motion are derived using the Spectral Finite Element Method, as detailed in Silva and Castello [15], and take the form of a system of Linear Ordinary Differential Equations (ODEs) as follows:

$$\mathbb{M}\ddot{\mathbf{u}} + \mathbb{K}\mathbf{u} = \mathbf{f}(t), \tag{2}$$

where $\mathbf{u}(t) \in \mathbb{R}^n$ is the displacement vector of the discrete governing equations.

The direct problem consists of determining the system response given a damage field $d(\boldsymbol{x}|\boldsymbol{\alpha})$. In that sense, to construct the forward model, equation (1) is discretized using $N_e = 120$ spectral elements of order $N_O = 6$, resulting in a system of $ngdl = 720$ degrees of freedom. The ODEs in (2) are then integrated with the Composite Explicit Method proposed by Kim and Lee [10], with a time step $\delta t = 5 \times 10^{-8} s$ over a time span of $T = 2 \times 10^{-3} s$.

In this study, damage is modeled as a scalar-valued 1D field $d(\mathbf{x}, \boldsymbol{\alpha}) : \mathbf{x} \in [0, L] \mapsto [0, 1]$, stationary in time, corresponding to a local reduction in stiffness; damage is parameterized by $\boldsymbol{\alpha} = (x_c, d\ell, D)$, as given by eq. (3):

$$d(x, \boldsymbol{\alpha}) = \begin{cases} D, & |x - x_c| \leq d\ell/2 \\ 0, & \text{otherwise} \end{cases}, \tag{3}$$

where x_c is the location of the damage's center, $d\ell$ is its width and D represents the local reduction in the Young's Modulus of the bar, that is to say $E(\mathbf{x}) = (1 - d(\mathbf{x}))E_0$. This simple model is commonly used in the literature, as can be seen in [14, 22, 12, 16, 3, 17, 9]. The properties of the intact material are provided in Table 1, along with the uncertainties associated with each parameter.

The uncertainty values for the properties, presented in Table 1, indicate that each model parameter can vary from its nominal value by an amount of *nominal value* $\times$ *uncertainty* $\times \gamma$ for each generated sample of the model. Here, $\gamma \sim \mathcal{N}(0, 1)$ represents a sample from an univariate Gaussian distribution with mean $\mu = 0$ and standard deviation $\sigma = 1$.

Table 1: Physical system properties and their associated uncertainties.

Parameters	Nominal Values	Considered Uncertainties
L	1 $[m]$	0.1%
A	3.6×10^{-5} $[m^2]$	1%
E	200×10^{9} $[Pa]$	2%
ρ	7556 $[kg/m^3]$	2%
F_0	10^4 $[N]$	-

2.2 Inverse Model - Bayesian Neural Network

The procedure for solving the inverse problem to recover the damage profiles from time-domain wave propagation data is based on a BNN framework. In a BNN, one or more model parameters $\boldsymbol{\theta} = (\mathbf{W}, \mathbf{b})$, where $\mathbf{W}$ represents the model weights and $\mathbf{b}$ denotes the biases, are treated probabilistically to account for uncertainties. This results in a model where the output is stochastic, as opposed to deterministic outputs in traditional NNs. In other words, while the conventional approach to NNs involves minimizing the model parameters through backpropagation, yielding a single deterministic value $\hat{\theta}_i$ for each parameter, the Bayesian approach aims to determine a probabilistic distribution for each parameter which uncertainty is accounted for [8, 4]:

$$\boldsymbol{\theta} \sim p(\boldsymbol{\theta}). \tag{4}$$

The first step in the process is to define the BNN architecture, as shown in Figure 1, considering a dropout rate of 5% in the dropout layers for the current problem. This architecture was optimized through hyperparameter tuning using a grid search approach. The search involved fine-tuning several hyperparameters of the deterministic layers, such as the layer types, the number of layers, and the number of units or filters in each layer. After this process, a series of layers (specifically, the last two layers in Figure 1) were incorporated into the architecture to handle the probabilistic nature of the model.

The network architecture presented in Figure 1 employs the *DenseReparameterization* layer as the layer immediately preceding the outputs, from *TensorFlow Probability* (version: 0.26.0-dev20250103). This layer incorporates trainable parameters for both weights and biases, while also allowing for the specification of a prior distribution. The prior for the layer parameters is set as a multivariate normal distribution with mean $\mu = 0$ and standard deviation $\sigma = 1$, and the posterior is modeled using a mean-field normal distribution. The divergence function, used for regularization during training, is defined with the Kullback-Leibler (KL) divergence, which measures the difference between the two distributions [7]:

$$\mathrm{KL}(q \,||\, p) = \frac{1}{N} \sum_{i=1}^{N} \left[\log \frac{q(\theta_i)}{p(\theta_i)} \right], \tag{5}$$

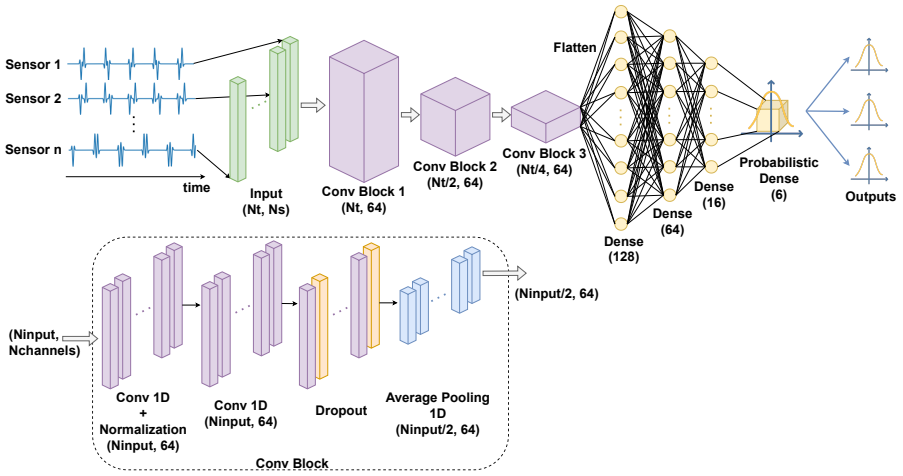

Fig. 1: Proposed architecture of the BNN. Here, N_s denotes the number of sensors used to measure the time-domain response, while N_t represents the number of time points, given the duration of the measurement.

where $q(\theta_i)$ and $p(\theta_i)$ represent the posterior and prior distributions of the parameters θ_i, respectively. Furthermore, the equation is normalized by the number of training samples N, ensuring that the divergence is averaged over the dataset.

The final output of the network is generated through the *IndependentNormal* layer. This layer models the output distribution, where the event shape corresponds to the number of independent normal variables. The distribution is then sampled, converting it into a tensor for downstream processing.

Regarding the loss function, the Negative Log-Likelihood $\mathcal{L}(\boldsymbol{\theta})$ is used [11]:

$$\mathcal{L}(\boldsymbol{\theta}) = -\sum_{i=1}^{n} \log p(\alpha_i \mid y_i, \boldsymbol{\theta}) \tag{6}$$

where, in the context of the approached problem, α_i are samples of the damage profile parameters (or the outputs of the model), y_i denotes the samples of observed time-domain data collected from the sensors (or the inputs of the model) and $p(\alpha_i \mid y_i, \theta)$ is the likelihood of the damage profile parameters α_i given the model parameters θ.

As for the optimization algorithm used during the backpropagation procedure of the proposed model, two were considered: the Adaptative Moment Estimation (ADAM) and the Stochastic Gradient Descent (SGD). Experiments were conducted with both algorithms, and the differences in their performance for minimizing the cost function will be discussed in Section 4, where the results are presented and discussed.

It is important to note here that, when using a BNN for prediction, the output is typically obtained using a Markov Chain Monte Carlo (MCMC) approach.

In this method, a large set of parameters θ_i is sampled from the posterior distribution and used to compute a series of possible outputs α_i. These outputs correspond to samples from the marginal distribution $p(\boldsymbol{\alpha}|\mathbf{y}, \boldsymbol{\theta})$, where $\mathbf{y}$ corresponds to the current measurement of the system [8].

In the context of the proposed problem, given a set of system responses $\mathbf{y}$, a sufficient number of samples are drawn to estimate the underlying distribution of the parameters $\boldsymbol{\alpha}$, which describe the damage field. The measured responses $\mathbf{y}$ consist of time-domain displacement history data in the $x-$direction, obtained from N_s sensors uniformly spaced along the length of the bar. Furthermore, samples that lack physical meaning — i.e., those that fall outside the domain of the damage parameters considered in the problem — are discarded during the inference sampling procedure.

3 Datasets

Synthetic data are simulated using the forward model discussed in Section 2.1, with an excitation and a damage profile as inputs. Narrowband signals are recognized as the preferred method for exciting Guided Wave signals in Non-Destructive Testing applications [19, 18]. Thus, for this study, a 2-cycle Hanning-windowed tone burst with a central frequency $f_c = 25$ kHz is used as the excitation $f(t)$; this excitation and its spectrum are shown in Figure 2.

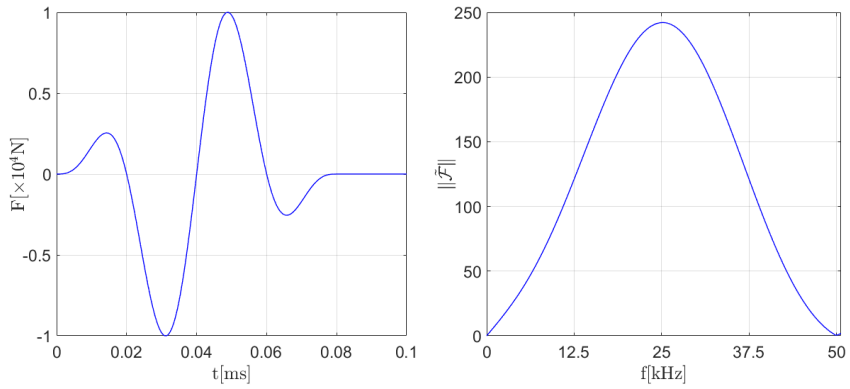

(a) Time domain (b) Frequency Domain

Fig. 2: Two-cycle Hanning-windowed pulse. (a) Time domain signal $F(t)$. (b) Absolute value of the Fourier transform of the signal $F(t)$.

This excitation signal, depicted in Figure 2, serves as the input to the forward model, which is used to solve the direct problem for two distinct scenarios. These scenarios, along with the dataset division for training and evaluating the BNN model, are presented in Table 2.

Table 2: Dataset division for training and evaluating the BNN model.

Dataset	Damage Profile	Properties Uncertainties?	Number of Samples
Training	Rectangular	No	20000
Validation/Test	Rectangular	Yes	5000

For each scenario, a damage profile is randomly generated, fully characterized by three parameters: position (center), size (width), and magnitude. The minimum and maximum values for each of these parameters are presented in Table 3.

Table 3: Damage profiles parameters and their limits.

Parameters	Minimum Value	Maximum Value
Position $[m]$	0.01	0.99
Size $[m]$	0.05	0.15
Magnitude	0.1	0.5

Furthermore, additional care is taken to ensure that the damage does not exceed the physical spatial domain. Specifically, the extent of the damage, considering both its position and size, is constrained to stay within the bar's length. For instance, if a damage profile is located at $0.01m$ on the bar and has a size of $0.1m$, it will not extend beyond the left end of the bar (at $x = 0m$). In such cases, the portion of the damage that exceeds the physical domain is disregarded, and a parameterization correction is applied to adjust its position and size accordingly.

The displacement field is measured by eight sensors over a period of 2 ms, with data sampled at $f_s = 400$ kHz. As discussed in Section 2.2, these sensor readings capture the system response in the time domain and serve as input to the inverse model, as shown in Figure 1. Therefore, the inputs and outputs of the BNN have shapes of *(number of samples, points in time, number of sensors)* and *(number of samples, number of damage parameters)*, respectively.

4 Results

In this section, the results are presented and discussed regarding the performance of the proposed BNN model in recovering damage field profiles, along with some challenges associated with training the BNN itself. First, it is important to note that the only preprocessing step applied to the raw data was normalizing both the input and output data to the range $[0, 1]$. Additionaly, training a BNN is a non-trivial task. In comparison to traditional NNs, there is a higher risk of falling into a poor local minimum, which is directly correlated with the optimization algorithm used for backpropagation. This issue can be explained by the fact that the Bayesian posterior for complex models, such as artificial NNs, is a high-dimensional and highly non-convex probability distribution [8]. In that sense,

the SGD optimizer has a more stable behavior regarding the convergence of the loss function to be minimized than the Adam.

Figure 3 illustrates examples of the damage profile recoveries from the BNN model considering 1000 samples drawn from the model's output for each test/validation sample (see Tables 1 and 3).

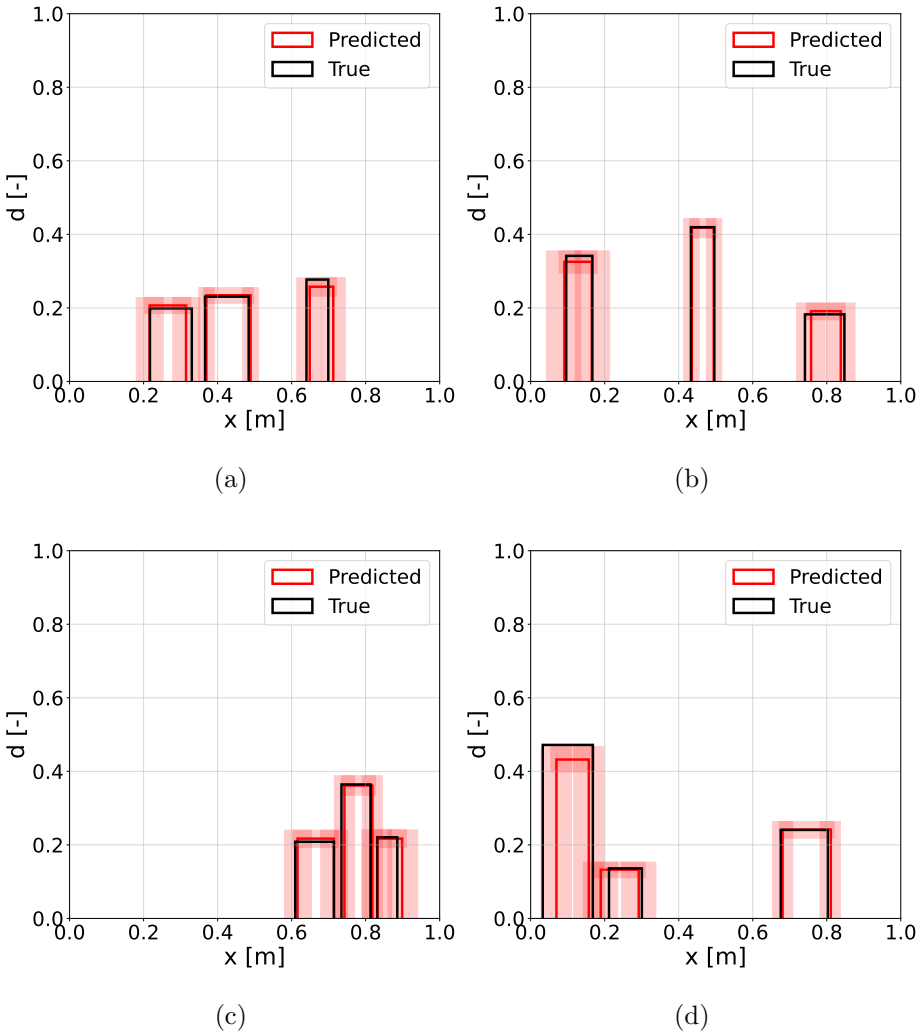

Fig. 3: Examples of damage profiles estimated with the BNN approach. The black continuous line represents the true damage profile, while the red continuous line is the mean of the predicted damage profile, accompanied by a 95% confidence envelope.

For the most of analyzed cases, a good agreement was achieved between the predicted damage fields of the BNN and the target values.

5 Conclusions

In the analysis of 1D wave propagation in an elastic bar, the behavior of a BNN applied to regression was investigated to model a simple damage field by estimating the probability distributions of the parameters that fully characterize the damage. This approach provides an alternative to estimating parameters within an inverse problem framework, effectively creating a surrogate model for inversion that offers enhanced analytical capabilities compared to deterministic NNs. For instance, when dealing with uncertainty and incorporating probabilistic reasoning, a digital twin could benefit from the stochastic nature of a BNN—something a deterministic model cannot provide [23].

The proposed inverse surrogate was evaluated in relation to test data that included uncertainties in the physical system properties, showing good agreement with respect to the predicted damage fields and the targets. The SGD optimizer was found to be significantly more stable than Adam (which heavily depends on the proper initialization of trainable parameters). The authors recommend further investigations with real-world data to assess how noise, measurement inaccuracies, and model errors might affect the performance of the proposed approach.

References

1. Arangio, S., Bontempi, F.: Structural health monitoring of a cable-stayed bridge with bayesian neural networks. Structure and Infrastructure Engineering **11**(4), 575–587 (2015)
2. Cha, Y.J., Ali, R., Lewis, J., Büyükztürk, O.: Deep learning-based structural health monitoring. Automation in Construction **161**, 105328 (2024)
3. Chen, C.T., Gu, G.X.: Learning hidden elasticity with deep neural networks. Proceedings of the National Academy of Sciences **118**(31), e2102721118 (2021)
4. Goan, E., Fookes, C.: Bayesian neural networks: An introduction and survey. In: Case Studies in Applied Bayesian Data Science: CIRM Jean-Morlet Chair, Fall 2018, pp. 45–87. Springer (2020)
5. Graff, K.F.: Wave motion in elastic solids. Courier Corporation (2012)
6. Hlaing, N., Morato, P.G., Santos, F.d.N., Weijtjens, W., Devriendt, C., Rigo, P.: Farm-wide virtual load monitoring for offshore wind structures via bayesian neural networks. Structural Health Monitoring **23**(3), 1641–1663 (2024)
7. Ji, S., Zhang, Z., Ying, S., Wang, L., Zhao, X., Gao, Y.: Kullback–leibler divergence metric learning. IEEE transactions on cybernetics **52**(4), 2047–2058 (2020)
8. Jospin, L.V., Laga, H., Boussaid, F., Buntine, W., Bennamoun, M.: Hands-on bayesian neural networks—a tutorial for deep learning users. IEEE Computational Intelligence Magazine **17**(2), 29–48 (2022)
9. Junqueira, B.F., Leiderman, R., Castello, D.A.: Damage recovery in composite laminates through deep learning from acoustic scattering of guided waves. Ultrasonics **139**, 107293 (2024)

10. Kim, W., Lee, J.H.: An improved explicit time integration method for linear and nonlinear structural dynamics. Computers & Structures **206**, 42–53 (2018)
11. Lampinen, J., Vehtari, A.: Bayesian approach for neural networks—review and case studies. Neural networks **14**(3), 257–274 (2001)
12. Lu, Z., Law, S.: Differentiating damage effects in a structural component from the time response. Mechanical systems and signal processing **24**(8), 2914–2928 (2010)
13. Luo, K., Zhu, J., Li, Z., Zhu, H., Li, Y., Hu, R., Fan, T., Chang, X., Zhuang, L., Yang, Z.: Ultrasonic lamb wave damage detection of cfrp composites using the bayesian neural network. Journal of Nondestructive Evaluation **43**(2), 48 (2024)
14. Moaveni, B., Behmanesh, I.: Effects of changing ambient temperature on finite element model updating of the dowling hall footbridge. Engineering Structures **43**, 58–68 (2012)
15. Silva, G.L., Castello, D.A.: Parametric reduced order models for wave propagation in 1d media containing defects. Journal of Sound and Vibration **558**, 117771 (2023)
16. Silva, G.L., Castello, D.A., Borges, L., Kaipio, J.P.: Damage identification in plates under uncertain boundary conditions. Mechanical Systems and Signal Processing **144**, 106884 (2020)
17. Silva, G.L., Castello, D.A., Kaipio, J.P.: Damage identification under uncertain mass density distributions. Computer Methods in Applied Mechanics and Engineering **376**, 113672 (2021)
18. Su, Z., Ye, L., Lu, Y.: Guided lamb waves for identification of damage in composite structures: A review. Journal of sound and vibration **295**(3-5), 753–780 (2006)
19. Takiy, A.E., Kitano, C., Higuti, R.T., Granja, S.C., Prado, V.T., Elvira, L., Martínez-Graullera, O.: Ultrasound imaging of immersed plates using high-order lamb modes at their low attenuation frequency bands. Mechanical Systems and Signal Processing **96**, 321–332 (2017)
20. Vashisht, R., Viji, H., Sundararajan, T., Mohankumar, D., Sumitra, S.: Structural health monitoring of cantilever beam, a case study—using bayesian neural network and deep learning. In: Structural Integrity Assessment: Proceedings of ICONS 2018, pp. 749–761. Springer (2019)
21. Vega, M.A., Todd, M.D.: A variational bayesian neural network for structural health monitoring and cost-informed decision-making in miter gates. Structural Health Monitoring **21**(1), 4–18 (2022)
22. Venanzi, I., Kita, A., Cavalagli, N., Ierimonti, L., Ubertini, F., et al.: Continuous oma for damage detection and localization in the sciri tower in perugia, italy. In: Proceedings of the International Operational Modal Analysis Conference (IOMAC 2019). pp. 127–136. Unknown (2019)
23. Yang, J., Langley, R.S., Andrade, L.: Digital twins for design in the presence of uncertainties. Mechanical Systems and Signal Processing **179**, 109338 (2022)
24. Yu, H., Seno, A.H., Sharif Khodaei, Z., Aliabadi, M.F.: Structural health monitoring impact classification method based on bayesian neural network. Polymers **14**(19), 3947 (2022)